CHAPTER-04

VIBRATIONS OF PHASE-LAGS ON ELECTRO-MAGNETO NONLOCAL ELASTIC SOLID WITH VOIDS IN GENERALIZED THERMOELASTIC CYLINDER/DISK

4.1 Introduction

In this chapter, the stress–strain–temperature relations, strain–displacement relations and governing equations have been addressed for electro-magneto transversely isotropic nonlocal elastic hollow cylinder with voids in the reference of three-phase-lag effect of heat conduction. The strength of the magnetic field proceeds in the direction of the z-axis of the hollow cylinder/disk. The simultaneous differential equations have been eliminated by applying elimination technique to obtain unknown field functions such as dilatation, equilibrated voids volume fraction, temperature, displacement and stresses. Free vibration analysis has been explored by applying stress free and thermally insulated/isothermal boundaries. Analytical results are verified by employing numerically analyzed results for unknown field functions and presented graphically for the vibrations of stress free field functions such as damping, frequencies and frequency-shift. The results have been authenticated by analyzing analytical and numerical results with existing literature with earlier published work. The study of present chapter based on three-phase-lag (TPL) model of generalized thermoelasticity may receive better approach to allow voids and relaxation time parameters, which have many applications in the field of science, technology and engineering. The study may also be useful in the area of seismology for mining and drilling in the earth’s crust.

4.2 The basic fundamental equations and mathematical model

Here a transversely isotropic nonlocal magneto-thermoelastic hollow cylinder with voids material of TPL model has been presented in the reference of generalized thermoelasticity. The inner and outer radii of hollow cylinder are assumed as $R_I = a$, $R_O = a\eta$ with the domain $a \le r \le a\eta$ and the surfaces are considered free from internal and external mechanical/thermal loads. The hollow cylinder is considered perfectly conductive and initially at undisturbed state with uniform temperature T_0. The strength of magnetic field $\boldsymbol{H}$ and cylindrical coordinates (r, θ, z) proceeds in z direction of the axis. The field components are displacement vector $\boldsymbol{u} = (u_r, u_\theta, u_z)$ where $u_\theta = 0, u_z = 0, u_r = u(r,t)$, concentration of voids volume fraction $\varphi = \varphi(r,t)$ and temperature component $T = T(r,t)$. Following Cowin and Nunziato(1983), Das et al. (2013) and Dhaliwal and Singh(1980), the Maxwell's equations in the absence of charge density and displacement current, with the impact of electromagnetic field, the equation of motion, equation of voids equilibrated volume fraction, and heat conduction equation without body forces and heat sources are given as

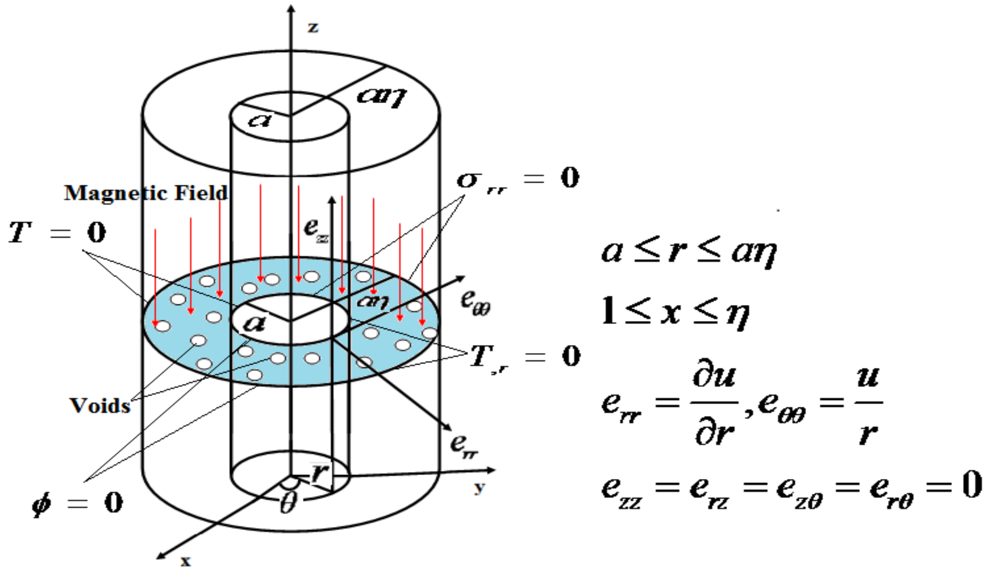

Figure 4.1 Geometry of the problem

Strain-displacement relations

$$e_{ij} = \frac{1}{2}(u_{i,j} + u_{j,i}), \tag{4.1}$$

where e_{ij}; $(i, j = r, \theta, \phi)$ are strain components, $\boldsymbol{u} = (u_r, 0, 0)$ is displacement vector.

Local–nonlocal stress relations

$$\left(1 - \zeta^2 \left(\frac{\partial^2}{\partial r^2} + \frac{1}{r}\frac{\partial}{\partial r}\right)\right)\sigma_{ij} = \sigma_{ij}^L \quad (i, j = r, \theta). \tag{4.2}$$

Here the quantities having superscript $"L"$ stands for the local medium, $\zeta = e_0 a_0$ is non local parameter, where a_0 is internal characteristic length and e_0 is material constant, σ_{ij}; $(i, j = r, \theta)$ are stress components, also $\sigma_{ij} = \sigma_{ij}^L$.

Constitutive relations

$$\left(1-\zeta^2\left(\frac{\partial^2}{\partial r^2}+\frac{1}{r}\frac{\partial}{\partial r}\right)\right)\sigma_{ij} = c_{ij}e_{kl} + b_{ij}\varphi - \beta_{ij}T \,. \tag{4.3}$$

Here $\beta_{ij}\,;(i, j = r, \theta)$ is the components of thermal modulii where $\beta_r = \beta_\theta = (c_{11}+c_{12})\alpha_1 + c_{13}\alpha_3$; $\alpha_1 = \alpha_3 = \alpha_T$ is coefficient of linear thermal expansion (Dhaliwal and Singh (1980)), T is assumed as increase in the reference temperature T_0 of the medium, $b_{ij} = b$ is the voids parameter, φ is the void volume fraction.

Modified Fourier's law

By introducing three phase-lags, namely thermal displacement gradient t_v, heat flux t_q and temperature gradient t_T, the classical Fourier law $\vec{q} = -K\vec{\nabla}T$ has been modified as given below:

$$\vec{q}_i(P,\, t+t_q) = -\left(K\vec{\nabla}T\,(P,\, t+t_T) + K^*\vec{\nabla}v(P, t+t_v)\right), \tag{4.4}$$

where K, K^* and $\vec{\nabla}v$ are thermal conductivity, additional material constant of characteristic theory, thermal displacement gradient, q_i are the heat flux vector components.

The entropy strain-temperature-voids relations

$$\rho S = \frac{\rho C_e}{T_0}T + \beta_{ij}e_{ij} + M\varphi \,, \tag{4.5}$$

where ρ is mass density, S is entropy per unit mass, M is thermo-void coupling parameter, C_e is specific heat at constant strain.

The equilibrated force balance equation

$$\rho\chi\left(1-\zeta^2\left(\frac{\partial^2}{\partial r^2}+\frac{1}{r}\frac{\partial}{\partial r}\right)\right)\frac{\partial^2\varphi}{\partial t^2} - h_{i,j} = -b_{ij}e_{ij} - \left(\xi_1 + \xi_2\frac{\partial}{\partial t}\right)\varphi + MT \,. \tag{4.6}$$

The relation between volume fraction gradient and equilibrated stress vector

$$h_i = \alpha_{ij}\varphi_{,i}\,, \tag{4.7}$$

where χ is the equilibrated inertia, ξ_1, ξ_2 are the material constants of voids, h_i is equilibrated stress vector, $\alpha_{ij} = \alpha$ is the void parameters.

The energy equation

$$\rho\frac{\partial S}{\partial t}T_0 = -q_{i,i} \quad , \tag{4.8}$$

where S is entropy per unit mass.

Equation of small motion in tensor form

$$\sigma_{ij,j} + F_i = \rho\left(1-\zeta^2\left(\frac{\partial^2}{\partial r^2}+\frac{1}{r}\frac{\partial}{\partial r}\right)\right)\frac{\partial^2 u}{\partial t^2}\,. \tag{4.9}$$

Here $\boldsymbol{F}_i;(i = r,\theta,z)$ are the components of body force $\boldsymbol{F} = (\boldsymbol{J}\times\boldsymbol{B})$. If ν is Poisson ratio and E is Young's modulus, then elastic constants are $c_{11} = \dfrac{E(1-\nu)}{(1+\nu)(1-2\nu)}$, $c_{12} = \dfrac{E\nu}{(1+\nu)(1-2\nu)}$.

The Maxwell's equations

The Maxwell's equations have been generated by electro-magnetic field in the absence of charge density and displacement current as:

$$\nabla\times\boldsymbol{E} = -\frac{\partial \boldsymbol{B}}{\partial t}\,,\quad \nabla\times\boldsymbol{H} = \boldsymbol{J}\,,\quad \boldsymbol{B} = \mu_e\boldsymbol{H}\,,\quad \nabla.\boldsymbol{B} = 0\,, \tag{4.10}$$

The generalized Ohm's law in continua of deformation is

$$\boldsymbol{J} = \sigma(\boldsymbol{E} + \frac{\partial u}{\partial t}\times\boldsymbol{B})\,. \tag{4.11}$$

Here $\boldsymbol{J}$ is current density, which is neglected due to small effect of temperature gradient. The strength of magnetic field $\boldsymbol{H} = \boldsymbol{H}_0 + h$, where $\boldsymbol{H}_0 = (0,0,H_0)$, h is perturbation of magnetic field which is very small due to the product of u and h and their derivatives might be neglected due to linearization of basic equations. Therefore, from equations (4.1)–(4.11), constitutive relations, the governing field equations are given as:

$$\left(\frac{\partial^2 u}{\partial r^2}+\frac{1}{r}\frac{\partial u}{\partial r}-\frac{u}{r^2}\right)-\frac{\rho}{c_{11}}\left(1-\zeta^2\left(\frac{\partial^2}{\partial r^2}+\frac{1}{r}\frac{\partial}{\partial r}\right)\right)\frac{\partial^2 u}{\partial t^2}+\frac{b}{c_{11}}\frac{\partial\varphi}{\partial r}-\frac{\beta_r}{c_{11}}\frac{\partial T}{\partial r}+\frac{1}{c_{11}}\boldsymbol{F}_{,r}=0\,, \tag{4.12}$$

$$-be+\alpha\nabla^2\varphi-\left(\xi_1+\xi_2\frac{\partial}{\partial t}\right)\varphi+\rho\chi\left(1-\zeta^2\left(\frac{\partial^2}{\partial r^2}+\frac{1}{r}\frac{\partial}{\partial r}\right)\right)\frac{\partial^2\varphi}{\partial t^2}+MT=0\,, \tag{4.13}$$

$$\begin{gathered}\left(\frac{\partial^2}{\partial t^2}+t_q\frac{\partial^3}{\partial t^3}+\frac{t_q^2}{2}\frac{\partial^4}{\partial t^4}\right)\left(\rho C_e T+T_0\left(\beta_r\frac{\partial u}{\partial r}+\beta_\theta\frac{u}{r}\right)+MT_0\varphi\right)\\ =\frac{1}{r}\frac{\partial}{\partial r}\left(r\frac{\partial T}{\partial r}\right)\left(K\left(\frac{\partial}{\partial t}+t_T\frac{\partial^2}{\partial t^2}\right)+K^*\left(1+t_v\frac{\partial}{\partial t}\right)\right)\end{gathered}, \tag{4.14}$$

$$\left.\begin{aligned}\left(1-\zeta^2\left(\frac{\partial^2}{\partial r^2}+\frac{1}{r}\frac{\partial}{\partial r}\right)\right)\sigma_{rr}&=c_{11}\frac{\partial u}{\partial r}+c_{12}\frac{u}{r}+b\varphi-\beta_r T\\ \left(1-\zeta^2\left(\frac{\partial^2}{\partial r^2}+\frac{1}{r}\frac{\partial}{\partial r}\right)\right)\sigma_{\theta\theta}&=c_{12}\frac{\partial u}{\partial r}+c_{11}\frac{u}{r}+b\varphi-\beta_\theta T\end{aligned}\right\}. \tag{4.15}$$

If the free vibration analysis is restricted to the transversely isotropic thermoelastic cylinder in radial direction, then using equations (4.10) and (4.11), the Lorentz force i.e. $F_r=(\boldsymbol{J}\times\boldsymbol{B})_{,r}$ in radial direction (Das et al. (2013)) , we obtained

$$F_r=\mu_e H_0^2\left(\frac{u}{r}+\frac{\partial u}{\partial r}\right),\;\; F_\theta=0\;\;,\;\; F_z=0\,, \tag{4.16}$$

Substituting values of Lorentz force from equation (4.16) in equation (4.12), we get

$$\left(\frac{\partial^2 u}{\partial r^2}+\frac{1}{r}\frac{\partial u}{\partial r}-\frac{u}{r^2}\right)-\frac{\rho(1-\zeta^2\nabla^2)}{c_{11}}\frac{\partial^2 u}{\partial t^2}+\frac{b}{c_{11}}\frac{\partial\varphi}{\partial r}-\frac{\beta_r}{c_{11}}\frac{\partial T}{\partial r}+\frac{\mu_e H_0^2}{c_{11}}\frac{\partial}{\partial r}\left(\frac{\partial u}{\partial r}+\frac{u}{r}\right)=0\,, \tag{4.17}$$

Taking divergence to both sides of equation (4.17) and rearranging it, we obtained

$$\left(1+\frac{\mu_e H_0^2}{c_{11}}\right)\nabla^2\left(\frac{1}{r}\frac{\partial}{\partial r}(ru)\right)-\frac{\rho}{c_{11}}(1-\zeta^2\nabla^2)\frac{\partial^2 e}{\partial t^2}+\frac{b}{c_{11}}\nabla^2\varphi-\frac{\beta_r}{c_{11}}\nabla^2 T=0\,, \tag{4.18}$$

where $\nabla^2=\frac{1}{r}\frac{\partial}{\partial r}\left(r\frac{\partial}{\partial r}\right)$.

The transversely isotropic TPL model generalized nonlocal magneto-thermoelastic hollow cylinder with voids material has been presumed to be undisturbed and at rest initially. Therefore, initial conditions are:

$$\frac{\partial u(r,0)}{\partial t}=\frac{\partial \varphi(r,0)}{\partial t}=\frac{\partial T(r,0)}{\partial t}=0\,,\; u(r,0)=\varphi(r,0)=T(r,0)=0, \quad \text{at} \quad r=a\,,\, a\eta. \tag{4.19}$$

The TPL model of generalized nonlocal magneto-thermoelastic hollow cylinder with voids is applied to stress free and equilibrated void volume fraction, thermally insulated/isothermal boundary conditions of domain $a \le r \le a\eta$. Hence, mathematically, we have:

Set I: $\frac{\partial T}{\partial r}=0 \;\; , \sigma_{rr}=0 \,, \;\varphi=0 \;\; ; \;\; r=a \;\; , \;\; r=a\eta\,.$ (4.20)

Set II: $T=0 \;\; , \;\sigma_{rr}=0 \,, \;\varphi=0 \;\; ; \;\; r=a \;\; , \;\; r=a\eta\,.$ (4.21)

4.3 Solution of the mathematical model

We set up the following non-dimensional parameters

$$\left.\begin{aligned}&(\tau_{XX}\,,\tau_{\theta\theta})=\frac{1}{c_{11}}(\sigma_{rr},\sigma_{\theta\theta}),\,(U,X,\zeta_0)=\frac{1}{a}(u,r,\zeta),(\tau,\tau_T,\tau_q,\tau_v)=\frac{c}{a}(t,t_T,t_q,t_v),\theta=\frac{T}{T_0},\\&\bar{\beta}_R=\frac{\beta_r T_0}{c_{11}},\;\bar{\beta}_\theta=\frac{\beta_\theta T_0}{c_{11}},\;\bar{b}^*=\frac{a^2\bar{b}}{\chi\Omega^{*2}},\bar{b}=\frac{b}{c_{11}},c_0=\frac{c_{12}}{c_{11}},\,c=\sqrt{\frac{c_{11}}{\rho}},\;\phi=\frac{\chi\Omega^{*2}}{a^2}\varphi,\;\bar{\xi}=\frac{c}{a}\frac{\xi_2}{\xi_1},\end{aligned}\right\}. \tag{4.22}$$

Using non-dimensional quantities as proposed in equation (4.22) in equations. (4.13) - (4.15) and (4.18), we attain following equations in non-dimensional form:

$$\left.\begin{aligned}\tau_{XX}&=\tau^L_{XX}=\frac{\partial U}{\partial X}+c_0\frac{U}{X}+\bar{b}^*\phi-\bar{\beta}_R\theta\\\tau_{\theta\theta}&=\tau^L_{\theta\theta}=c_0\frac{\partial U}{\partial X}+\frac{U}{X}+\bar{b}^*\phi-\bar{\beta}_\theta\theta\end{aligned}\right\}, \tag{4.23}$$

$$R_h\nabla^2_X e+\bar{b}^*\nabla^2_X\phi-\bar{\beta}_R\nabla^2_X\theta=(1-\zeta_0^2\nabla^2_X)\frac{\partial^2 e}{\partial\tau^2}\,, \tag{4.24}$$

$$-a_2 e+\nabla^2_X\phi-a_1\left(1+\bar{\xi}\frac{\partial}{\partial\tau}\right)\phi+a_3\theta=(1-\zeta_0^2\nabla^2_X)\frac{1}{\delta_1^2}\frac{\partial^2\phi}{\partial\tau^2}\,, \tag{4.25}$$

$$\left(\frac{\partial^2}{\partial\tau^2}+\tau_q\frac{\partial^3}{\partial\tau^3}+\frac{\tau_q^2}{2}\frac{\partial^4}{\partial\tau^4}\right)\left(\Omega^*\theta+a_4 e+a_5\phi\right)=\left(\left(\frac{\partial}{\partial\tau}+\tau_T\frac{\partial^2}{\partial\tau^2}\right)+\bar{K}\left(1+\tau_v\frac{\partial}{\partial\tau}\right)\right)\left\{\frac{1}{X}\frac{\partial}{\partial X}\left(X\frac{\partial\theta}{\partial X}\right)\right\} \tag{4.26}$$

where

$$a_1 = \frac{\xi_1 a^2}{\alpha}, a_2 = \frac{b\chi\Omega^{*2}}{\alpha}, \; a_3 = \frac{M\chi\Omega^{*2}T_0}{\alpha}, \; a_4 = \frac{\varepsilon_T\Omega^*}{\overline{\beta}_R}, \; a_5 = \frac{Mca^3}{K\chi\Omega^{*2}}, \; \omega^* = \frac{c_{11}C_e}{K}, R_h = 1 + \frac{\mu_e H_0^2}{c_{11}},$$

$$\overline{K} = \frac{aK^*}{cK}, \; \Omega^* = \frac{a\omega^*}{c}, \; \varepsilon_T = \frac{T_0\beta_r^2}{\rho C_e c_{11}}, \; \delta_1^2 = \frac{\alpha}{\chi c_{11}}, \; e = \frac{1}{X}\left(\frac{\partial}{\partial X}(XU)\right), \nabla_X^2 = \frac{1}{X}\frac{\partial}{\partial X}\left(X\frac{\partial}{\partial X}\right).$$

Now we introduce the following time harmonics as proposed by Pierce (1981):

$$\left(\overline{e} \quad \overline{\phi} \quad \overline{\theta}\right) = (e \quad \phi \quad \theta)\exp(i\Omega\tau). \tag{4.27}$$

Here $\Omega = \omega a / c$ denotes circular frequency. Using proposed time harmonics from equation (4.27) in equations (4.23–4.26), we get

$$\begin{cases} \tau_{XX} = \overline{e} + \dfrac{c_0 - 1}{X}\overline{U} + \overline{b}^*\overline{\phi} - \overline{\beta}_R\overline{\theta} \\ \tau_{\theta\theta} = c_0\overline{e} + \left(\dfrac{1-c_0}{X}\right)\overline{U} + \overline{b}^*\overline{\phi} - \overline{\beta}_\theta\overline{\theta} \end{cases}, \tag{4.28}$$

$$\begin{cases} \left((R_h - \zeta_0^2\Omega^2)\nabla_X^2 + \Omega^2\right)\overline{e} + \overline{b}^*\nabla_X^2\overline{\phi} - \overline{\beta}_R\nabla_X^2\overline{\theta} = 0 \\ -a_2\overline{e} + \left(a_1^*\nabla_X^2 + \dfrac{(a_1 i\Omega\overline{\xi}^*\delta_1^2 + \Omega^2)}{\delta_1^2}\right)\overline{\phi} + a_3\overline{\theta} = 0 \\ \Omega^2\Omega^*\tau_q^*\overline{e} + \Omega^2\tau_q^* a_4\overline{\phi} + \left(a_2^*\nabla_X^2 - \Omega^2\tau_q^* a_5\right)\overline{\theta} = 0 \end{cases}, \tag{4.29}$$

where $a_1^* = \dfrac{\delta_1^2 - \zeta_0^2\Omega^2}{\delta_1^2}$, $a_2^* = (\Omega^2\tau_T^* - \overline{K}i\Omega\tau_v^*)$, $\overline{\xi}^* = i\Omega^{-1} - \overline{\xi}$,

$$\tau_q^* = \left(\Omega^{-2} + i\Omega^{-1}\tau_q - \frac{\tau_q^2}{2}\right), \; \tau_T^* = i\Omega^{-1} - \tau_T, \; \tau_v^* = i\Omega^{-1} - \tau_v.$$

For the solution of equation (4.29), we have non-trivial solution given as:

$$(\nabla_X^6 - L_1\nabla_X^4 + L_2\nabla_X^2 - L_3)(\overline{e}, \; \overline{\phi}, \; \overline{\theta}) = 0, \tag{4.30}$$

where $L_1 = \left(-\dfrac{\Omega^2}{R_h - \zeta_0^2\Omega^2} - \dfrac{a_1 i\Omega\overline{\xi}^*\delta_1^2 + \Omega^2}{\delta_1^2 a_1^*} + \dfrac{\Omega^2\tau_q^* a_5}{a_2^*} + \dfrac{\overline{b}^* a_2}{(R_h - \zeta_0^2\Omega^2)a_1^*} - \dfrac{\overline{\beta}_R\Omega^2\Omega^*\tau_q^*}{(R_h - \zeta_0^2\Omega^2)a_2^*} \right)$,

$$L_2 = \left(\begin{array}{l} \dfrac{\Omega^2(a_1 i\Omega\overline{\xi}^*\delta_1^2 + \Omega^2)}{(R_h - \zeta_0^2\Omega^2)\delta_1^2 a_1^*} - \dfrac{(a_1 i\Omega\overline{\xi}^*\delta_1^2 + \Omega^2)\Omega^2\tau_q^* a_5}{\delta_1^2 a_1^* a_2^*} - \dfrac{\Omega^2\Omega^2\tau_q^* a_5}{(R_h - \zeta_0^2\Omega^2)a_2^*} - \dfrac{a_3\Omega^2\tau_q^* a_4}{a_1^* a_2^*} + \\ \dfrac{\overline{b}^* a_2\Omega^2\tau_q^* a_5}{(R_h - \zeta_0^2\Omega^2)a_1^* a_2^*} + \dfrac{\overline{b}^* a_3\Omega^2\Omega^*\tau_q^*}{(R_h - \zeta_0^2\Omega^2)a_1^* a_2^*} + \dfrac{\overline{\beta}_R a_2\Omega^2\tau_q^* a_4}{(R_h - \zeta_0^2\Omega^2)a_1^* a_2^*} + \dfrac{\overline{\beta}_R\Omega^2\Omega^*\tau_q^*(a_1 i\Omega\overline{\xi}^*\delta_1^2 + \Omega^2)}{(R_h - \zeta_0^2\Omega^2)a_1^* a_2^*\delta_1^2} \end{array} \right),$$

$$L_3 = \left(\dfrac{\Omega^4(a_1 i\Omega\overline{\xi}^*\delta_1^2 + \Omega^2)\tau_q^* a_5}{(R_h - \zeta_0^2\Omega^2)\delta_1^2 a_1^* a_2^*} + \dfrac{\Omega^4\tau_q^* a_3 a_5}{(R_h - \zeta_0^2\Omega^2)a_1^* a_2^*} \right).$$

Since the solution of equation (4.30) is bounded for $X \to \infty$, therefore its roots must be positive real parts, i.e. $\mathrm{Re}(k_i) \geq 0,\ \forall\ i = 1,\ 2,\ 3)$. Therefore, the roots $k_i;\ i = 1,\ 2,\ 3$ of equation (4.30) are:

$$k_1 = \sqrt{\frac{1}{3}\left(2A\sin B + L_1\right)},\ k_2 = \sqrt{\frac{1}{3}\left(L_1 - A(\sqrt{3}\cos B + \sin B)\right)},\ k_3 = \sqrt{\frac{1}{3}\left(L_1 + A(\sqrt{3}\cos B - \sin B)\right)},$$

where, $A = \sqrt{L_1^2 - 3L_2}$, $C = -\dfrac{2L_1^3 - 9L_1L_2 + 27L_3}{2L_1^3}$, $B = \dfrac{1}{3}\sin^{-1}(C)$.

Hence after solving the characteristic equation (4.30) and on applying elimination technique, the complete solution obtained as

$$\left(\overline{\theta} \quad \overline{e} \quad \overline{\phi}\right) = \sum_{i=1}^{3}\left(1 \quad R_i \quad S_i\right)\left(P_i J_0(k_i X) + Q_i Y_0(k_i X)\right), \tag{4.31}$$

where, $R_i = R_{1i}/R_{2i}$, $S_i = -S_{1i}/S_{2i}$; $i = 1,\ 2,\ 3$,

$$R_{1i} = k_i^2\left(\frac{\overline{\beta}_R a_2}{(R_h - \zeta_0^2\Omega^2)a_1^*} - \frac{a_3}{a_1^*} \right) - \frac{\Omega^2 a_3}{(R_h - \zeta_0^2\Omega^2)a_1^*},$$

$$R_{2i} = k_i^4\left(\frac{\overline{\beta}_R}{R_h - \zeta_0^2\Omega^2} \right) + k_i^2\left(\frac{\overline{\beta}_R(a_1 i\Omega\overline{\xi}^*\delta_1^2 + \Omega^2)}{(R_h - \zeta_0^2\Omega^2)\delta_1^2 a_1^*} + \frac{\overline{b}^* a_3}{(R_h - \zeta_0^2\Omega^2)a_1^*} \right),$$

$$S_{1i} = k_i^2\left(\frac{\Omega^2\Omega^*\tau_q^*}{a_2^*} \right) + \left(\frac{(a_1 i\Omega\overline{\xi}^*\delta_1^2 + \Omega^2)\Omega^2\Omega^*\tau_q^*}{\delta_1^2 a_1^* a_2^*} + \frac{a_2\Omega^2\tau_q^* a_4}{a_1^* a_2^*} \right),$$

$$S_{2i}=k_i^4+\left(\frac{(a_1i\Omega\overline{\xi}^*\delta_1^2+\Omega^2)}{\delta_1^2a_1^*}-\frac{\Omega^2\tau_q^*a_5}{a_2^*}\right)k_i^2-\left(\frac{\Omega^2\tau_q^*a_5(a_1i\Omega\overline{\xi}^*\delta_1^2+\Omega^2)}{\delta_1^2a_1^*a_2^*}+\frac{a_3\Omega^2\tau_q^*a_4}{a_1^*a_2^*}\right).$$

Here P_i, Q_i; $i=1,\,2,\,3$ are arbitrary constants that depend on Ω only. J_0 and Y_0 are Bessel functions of First and Second kinds of order zero respectively. Resolving cubical dilation $(\overline{e})$ from equation (4.31) for displacement $\overline{U}$, we obtain

$$\overline{U}=\sum_{i=1}^{3}\frac{1}{k_i}R_i\left(P_iJ_1(k_iX)-Q_iY_1(k_iX)\right). \tag{4.32}$$

The temperature gradient has been obtained on differentiating the first part of equation (4.31) with respect to X, we obtain

$$\frac{\partial\overline{\theta}}{\partial X}=\sum_{i=1}^{3}k_i\left[P_iJ_1\left(k_iX\right)-Q_iY_1\left(k_iX\right)\right]. \tag{4.33}$$

On substitution of $\overline{e}\,,\overline{U}\,,\overline{\phi}\,,\overline{\theta}$ from equations (4.31–4.32) in equation (4.28), we get

$$\tau_{XX}=\sum_{i=1}^{3}\left(P_i\left\{\mathrm{H}_iJ_0(k_iX)+\left(\frac{c_0-1}{k_iX}\right)R_iJ_1(k_iX)\right\}+Q_i\left\{\mathrm{H}_iY_0(k_iX)-\left(\frac{c_0-1}{k_iX}\right)R_iY_1(k_iX)\right\}\right), \tag{4.34}$$

$$\tau_{\theta\theta}=\sum_{i=1}^{3}\left(P_i\left\{\mathrm{H}_i^*J_0(k_iX)-\left(\frac{c_0-1}{k_iX}\right)R_iJ_1(k_iX)\right\}+Q_i\left\{\mathrm{H}_i^*Y_0(k_iX)+\left(\frac{c_0-1}{k_iX}\right)R_iY_1(k_iX)\right\}\right), \tag{4.35}$$

where $\mathrm{H}_i=R_i+S_i\overline{b}^*-\overline{\beta}_R,\ \mathrm{H}_i^*=c_0R_i+S_i\overline{b}^*-\overline{\beta}_R,\quad i=1,2,3$.

4.4 Frequency relations

In this section, for the analysis of free vibrations, the frequency equations have been obtained for equations (4.31)–(4.34) for boundary conditions given in equations (4.20) and (4.21), at inner and outer radii $X=1$ and $X=\eta$. On simplification these equations, we obtain a system of homogenous equations given below

$$(\Pi_{ij})_{6\times6}\,(\mathrm{H})_{6\times1}=0\quad;\ i,j=1\ to\ 6, \tag{4.36}$$

where $\mathrm{H}=(P_1,\,P_2,\,P_3,\,Q_1,\,Q_2,\,Q_3)^T$. On solving equation (4.36) six linear homogeneous equations have been obtained with six unknowns. Therefore for non-trivial solution of equation (4.36), we must have

$$\left|\ \Pi_{ij}\right| = 0\ ; \quad i, j = 1\ to\ 6\,. \tag{4.37}$$

Here, the constants of Π_{ij} ; $i, j = 1\ to\ 6$ are defined for thermally insulated boundary conditions in set I and isothermal boundary conditions in set II given below:

Set I: The constant parameters of Π_{ij} ; $i, j = 1\ to\ 6$ are

$$\left.\begin{array}{l}\Pi_{1j} = \mathrm{H}_i J_0(k_i) + \left((c_0 - 1)/k_i\right) R_i J_1(k_i); \quad i, j = 1, 2, 3; \\ \Pi_{3j} = S_i J_0\left(k_i\right); \quad \Pi_{5j} = k_i J_1\left(k_i\right); \quad i, j = 1, 2, 3; \\ \Pi_{1j} = \mathrm{H}_i Y_0(k_i) - \left((c_0 - 1)/k_i\right) R_i Y_1(k_i);\ i = 1, 2, 3,\ j = 4, 5, 6 \\ \Pi_{3j} = S_i Y_0\left(k_i\right); \quad \Pi_{5j} = -k_i Y_1\left(k_i\right); i = 1, 2, 3;\ j = 4, 5, 6; \end{array}\right\}. \tag{4.38}$$

Set II: In this case, the elements of $\Pi_{1j}, \Pi_{2j}, \Pi_{3j}, \Pi_{4j}; j = 1\ to\ 6$, remain same as given in equation (4.38). The remaining elements of $\Pi_{5j}, \Pi_{6j}; j = 1\ to 6$,in equation (4.37) for stress free isothermal boundary condition are

$$\Pi_{5j} = J_0\left(k_i\right);\ i, j = 1, 2, 3, \quad \Pi_{5j} = Y_0\left(k_i\right);\ i = 1, 2, 3;\ j = 4, 5, 6;\}\,, \tag{4.39}$$

The elements of Π_{2j} , Π_{4j} , Π_{6j} ; $j = 1\ to\ 6$, are obtained by inserting η along with k_i , in the elements of Π_{1j} , Π_{3j} , Π_{5j} ; $j = 1\ to\ 6$.

4.5 Deduction of analytical results

4.5.1 Generalized transversely magneto-thermoelastic voids hollow cylinder

If the nonlocal constant is assumed to be absent, i.e. $\zeta_0 = 0$, then the analysis has been reduced to transversely isotropic magneto-thermoelastic voids hollow cylinder with the TPL model of generalized thermoelasticity.

4.5.2 Generalized and classical magneto-thermoelastic cylinder

If we establish thermal equilibrium and the nonlocal parameter and voids constants are ignored, i.e. $\zeta_0 = 0$, $\alpha = b = M = \xi_1 = \xi_2 = 0$, then the analysis has been reduced to the three-phase-lag model of generalized transversely isotropic electro-magneto-thermoelastic hollow cylinder, which completely agree with the analysis and governing equations of Das et al. (2013) . Again, if $t_q = t_v = t_T = 0$, then the analysis reduced to classical magneto-thermoelastic cylinder.

4.5.3 Generalized thermoelastic LS model transversely isotropic cylinder

Again, if the nonlocal parameter, magnetic field constants and voids constants are ignored i.e. $\zeta_0 = 0$, $\mu_e = H_0 = 0$ and $\alpha = b = M = \xi_1 = \xi_2 = 0$ and also $K^* = t_q = t_T = 0$, $t_v = t_0$, therefore the analysis reduced to transversely isotropic thermoelastic hollow cylinder whose governing equations and free vibration analysis agree with Sharma et al. (2022a) in the absence of functionally graded materials.

4.5.4 Elastic cylinder

If the constants i.e. the nonlocal, voids, magneto, relaxation times and thermo-mechanical parameters are removed i.e. $\zeta_0 = 0$, $\alpha = b = M = \xi_1 = \xi_2 = 0$, $\mu_e = H_0 = 0$, $K^* = t_q = t_v = t_T = 0$ and $T = \beta_R = \varepsilon_T = 0$, then the governing equations and the free vibration analysis have been reduced to transversely isotropic elastic cylinder which agree with Kele and Tutuncu in the absence of functionally graded materials.

4.6 Numerical results and discussion

The numerical computational results have been proposed to validate the analytical results for TPL model of nonlocal magneto-thermoelastic hollow cylinder with voids. The simulated results have been performed for generalized thermoelastic models, i.e. coupled thermoelasticity (CTE), Lord-Shulman (LS), dual-phase-lag (DPL) and three-phase-lag (TPL) in absence/presence of magnetic fields for nonlocal and local elastic materials with voids in thermoelastic hollow cylinder by taking the ratio of outer to inner radius $\eta = 1.5,\ 2.0$. For computation purpose the transversely isotropic material of single crystal of zinc thermoelastic solid with voids material has been assumed and its constant values are given in SI units (Chadwick and Seet (1970)):

$$K = 1.24\times10^{2} Wm^{-1}\deg^{-1}, C_e = 3.9\times10^{2} JKg^{-1}\deg^{-1},\ \rho = 7.14\times10^{3} Kg\, m^{-3},\ \chi = 1.753\times10^{-15} m^{2},$$
$$c_{11} = 1.628\times10^{11} Nm^{-2}, c_{12} = 1.562\times10^{11} Nm^{-2}, \beta_r = 5.75\times10^{6} Nm^{-2}\deg^{-1}, T_0 = 296K,\ \omega = 10,$$
$$\alpha = 3.688\times10^{-5} N, M = 2.0\times10^{6} Nm^{-2}\deg^{-2}, \xi_1 = \xi_2 = 1.475\times10^{10} Nm^{-2}, b = 1.13849\times10^{10} Nm^{-2}.$$

The three-phase-lag (TPL) parameters have been considered from Mondal and Kanoria (2020) as $t_v = 0.05$, $t_T = 0.07$, $t_q = 0.09$, $K^* = 7.0$. The magnetic field parameters have been assumed as $\mu_e = 4\pi \times 10^7 H/m$, $H_0 = 10^8 A/m$ from Othman and Hilal (2017). The nonlocal parameter value has been considered as $\xi_0 = 2.3102$ from Bachher and Sarkar (2019). The frequency dispersion relations have been attained from considered boundary conditions, which are transcendental equations, whose solution is in the form of complex numbers, is because of rate of dissipative term in heat conduction equation (4.4). The numerically analyzed computations and simulations have been applied to equation (4.37) for thermally insulated cases till four places of decimals.

The numerical Iteration method has been applied to evaluate the roots of the equation (4.37), which is of the type $g(\Omega) = 0$. The required substitution for the method i.e. $\Omega = \Phi(\Omega)$, so that the sequence (Ω_n) of iterations has been generated for desired accuracy level. If the condition $|\Phi'(\Omega)| \ll 1$, holds for all $\Omega \in I$, then the root of approximations will converge to the actual value $\Omega = \Omega_a$ of the root, provided $\Omega_0 \in I$, here I is the expected interval. The Iteration method's condition for numerical convergence is $|\Omega_{n+1} - \Omega_n| < \varepsilon$. Here ε has been considered small arbitrary number to achieve the accuracy level selected randomly, which may be satisfied. Therefore, this procedure is repeated continuously for the values of Ω until desired level of accuracy achieved. The numerically analyzed complex values (frequencies) of Ω might be written as $\Omega^m = \Omega_R^m + i\Omega_I^m$. The real and imaginary parts have been considered as natural frequencies $\Omega_R^m = \Omega_R$ and dissipation factor $\Omega_I^m = \Omega_I$ respectively. The value m has been considered as mode number, which corresponds to root of the equation. The numerically analyzed natural frequencies have been presented graphically for TPL, DPL, LS and CTE models of thermoelasticity for nonlocal/local thermoelastic hollow cylinder in presence and absence of magnetic field. The real parts have been assumed as natural frequencies (Ω_R) against mode number (m) for nonlocal as well as local elastic cylinder with and without magnetic field at $\eta = 1.5$ have been shown graphically in Fig. 4.1(a-b) to Fig. 4.2(a-b). These Figs. 4.1(a-b) to 4.2(a-b) (nonlocal and local case) depict that initially the vibrations are low and with increasing values of m, the variation of vibrations goes on increasing with increasing mode number. The behaviors of vibrations are lower in the presence of a magnetic field in contrast to the absence of magnetic field for nonlocal and local elastic materials. This is noticed from Figs. 4.1(a-b) and 4.2(a-b) that the behavior of variation of natural frequencies is larger in case of TPL model of generalized thermoelasticity in comparison with other models of thermoelasticity.

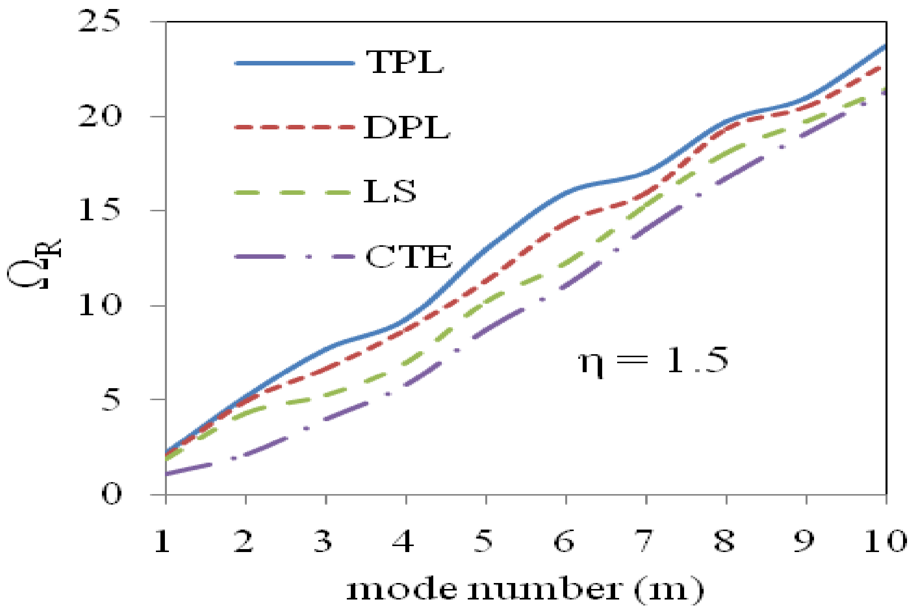

Figure 4.1(a): Natural frequencies (Ω_R) against mode number (m) for TPL, DPL, LS and CTE models at $\eta = 1.5$ in nonlocal thermoelastic cylinder with voids with magnetic field.

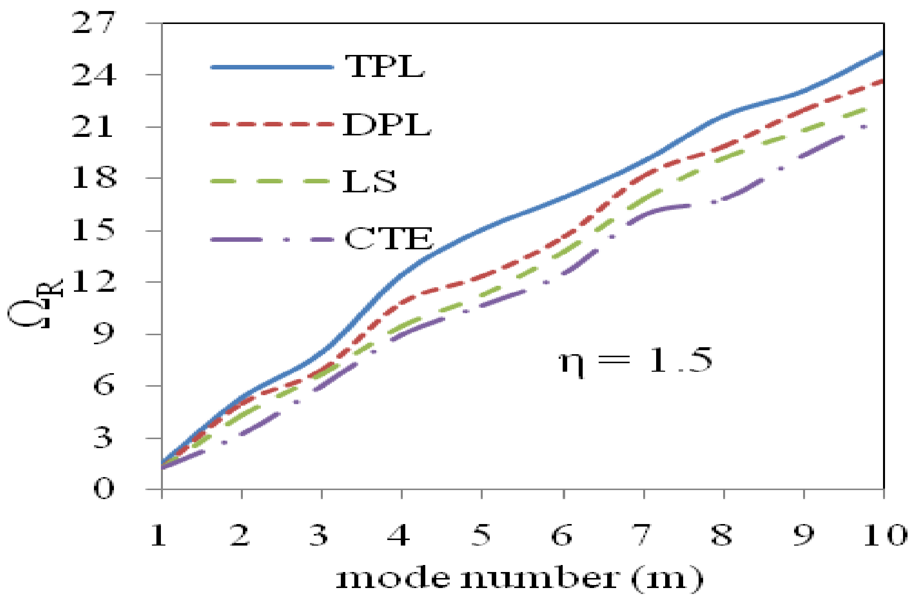

Figure 4.1(b): Natural frequencies (Ω_R) against mode number (m) for TPL, DPL, LS and CTE models at $\eta = 1.5$ in nonlocal thermoelastic cylinder with voids without magnetic field.

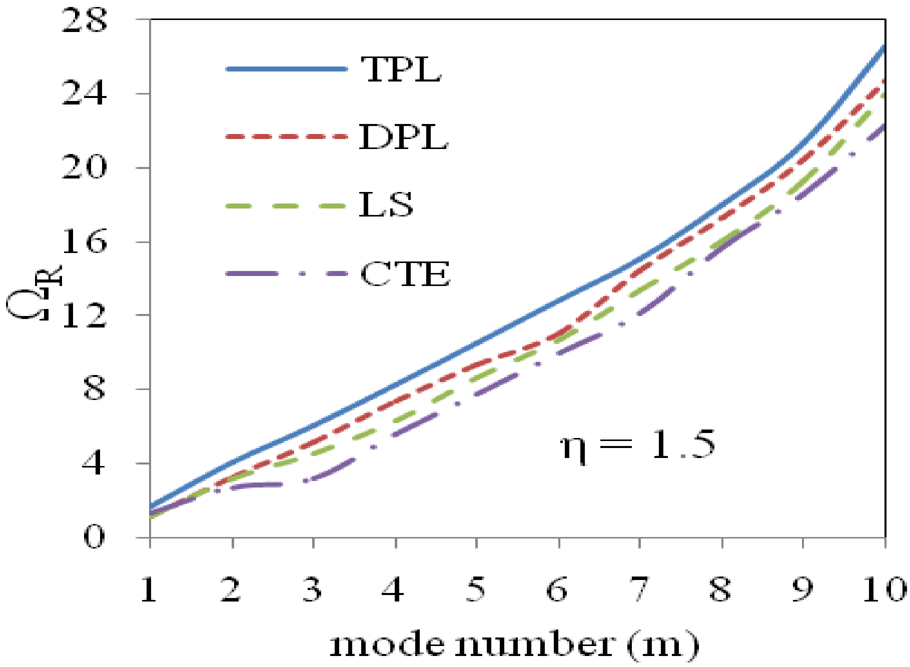

Figure 4.2(a): Natural frequencies (Ω_R) against mode number (m) for TPL, DPL, LS and CTE models at $\eta = 1.5$ in local thermoelastic cylinder with voids with magnetic field.

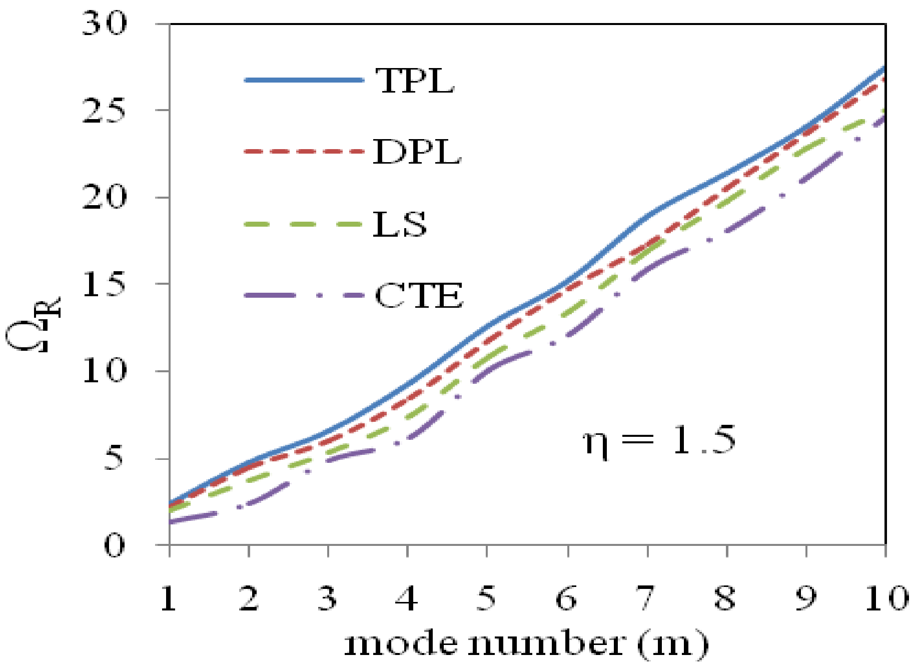

Figure 4.2(b): Natural frequencies (Ω_R) against mode number (m) for TPL, DPL, LS and CTE models at $\eta = 1.5$ in local thermoelastic cylinder with voids without magnetic field.

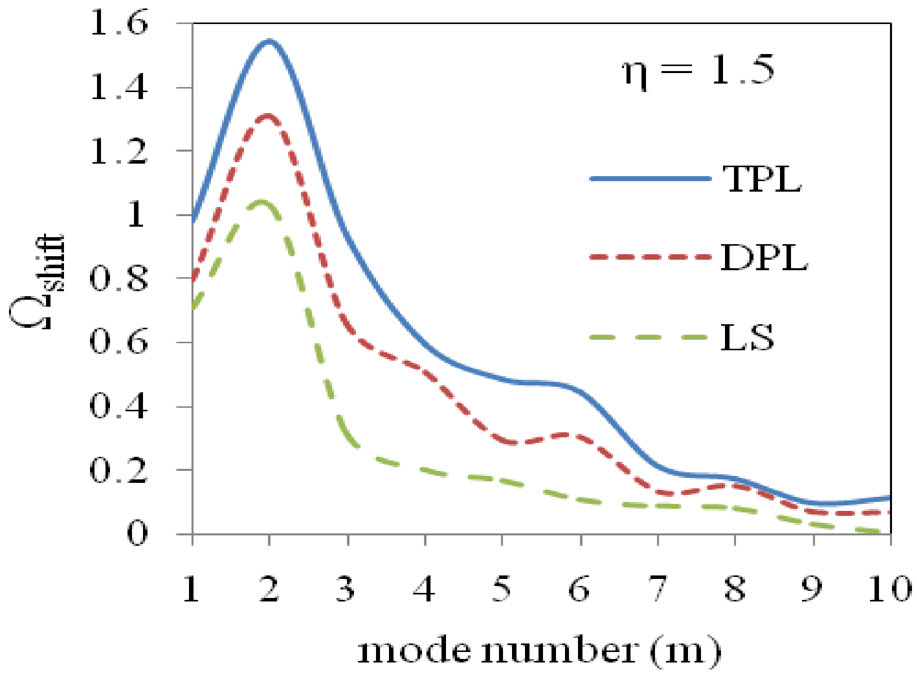

Figure 4.3(a): Frequency shift (Ω_{Shift}) against mode number (m) for TPL, DPL and LS models at $\eta = 1.5$ in nonlocal thermoelastic cylinder with voids with magnetic field.

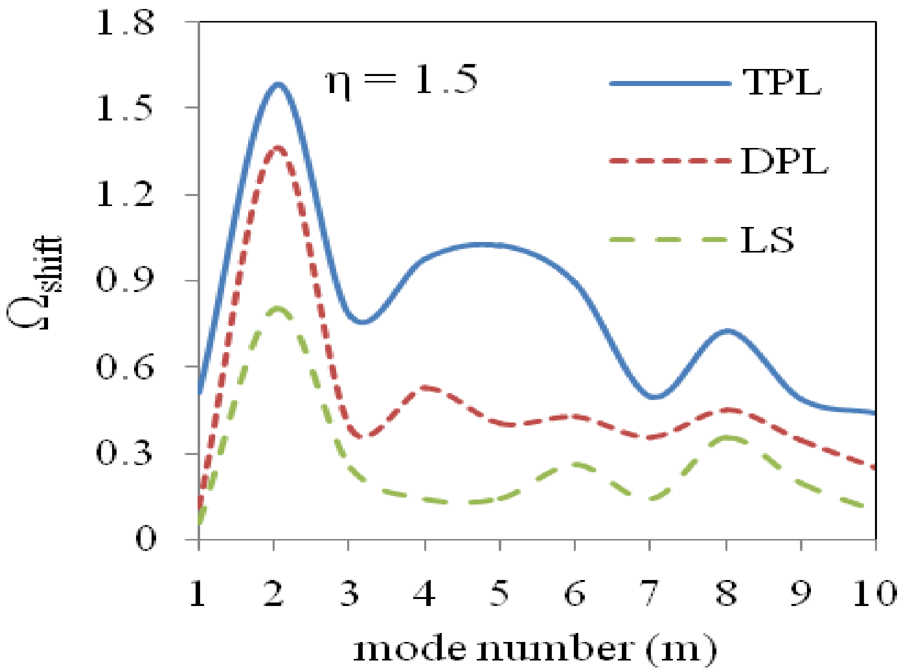

Figure 4.3(b): Frequency shift (Ω_{Shift}) against mode number (m) for TPL, DPL and LS models at $\eta = 1.5$ in nonlocal thermoelastic cylinder with voids without magnetic field.

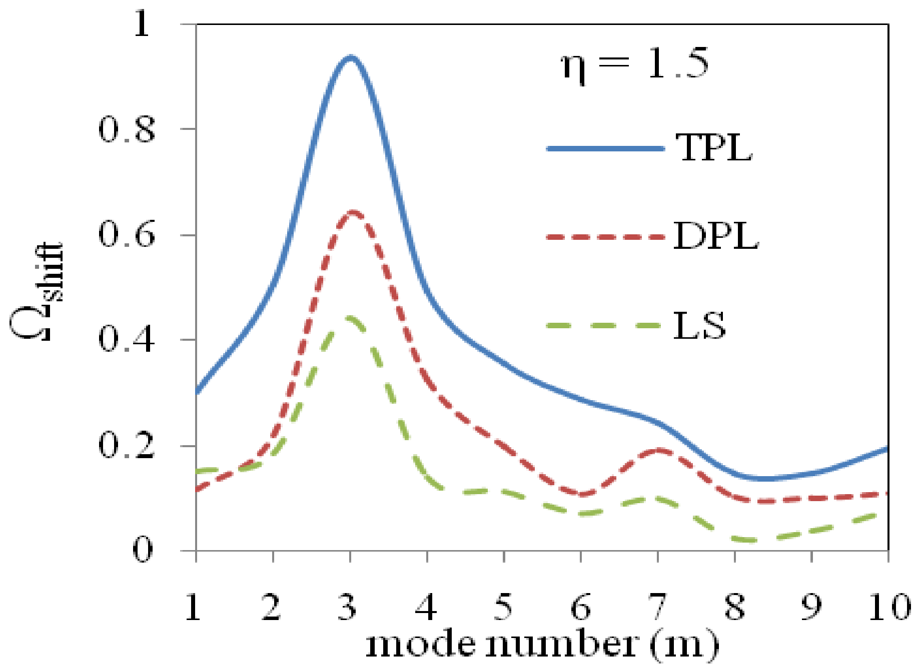

Figure 4.4(a): Frequency shift (Ω_{Shift}) against mode number (m) for TPL, DPL and LS models at $\eta = 1.5$ in local thermoelastic cylinder with voids with magnetic field.

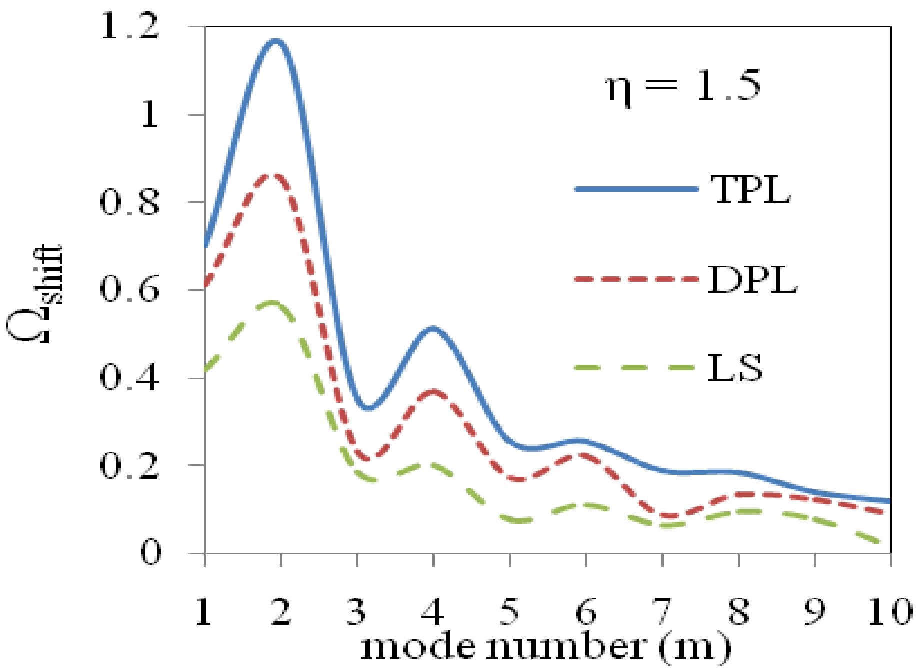

Figure 4.4(b): Frequency shift (Ω_{Shift}) against mode number (m) for TPL, DPL and LS models at $\eta = 1.5$ in local thermoelastic cylinder with voids without magnetic field.

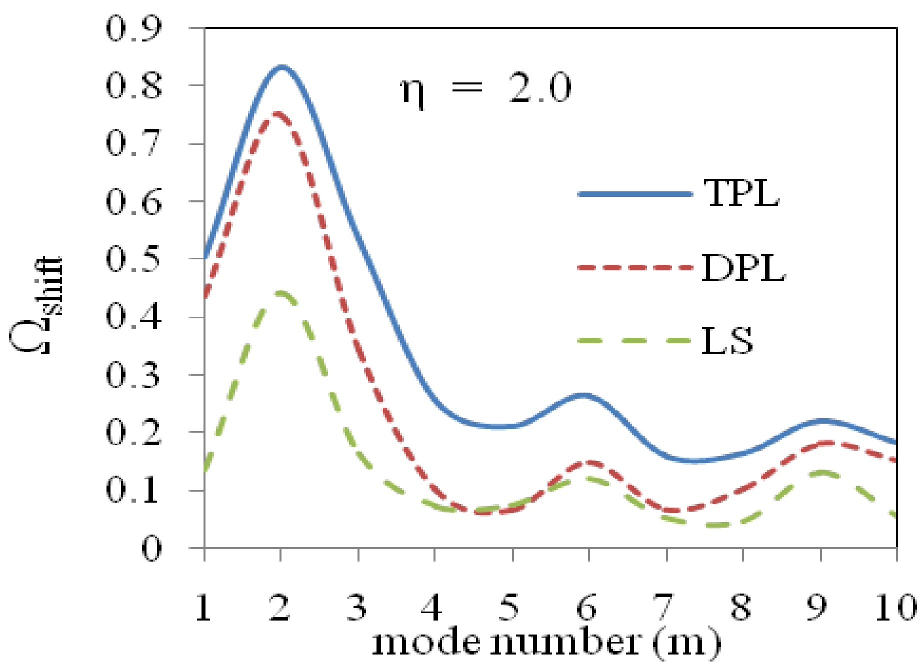

Figure 4.5(a): Frequency shift (Ω_{Shift}) against mode number (m) for TPL, DPL and LS models at $\eta = 2.0$ in nonlocal thermoelastic hollow cylinder with voids with magnetic field.

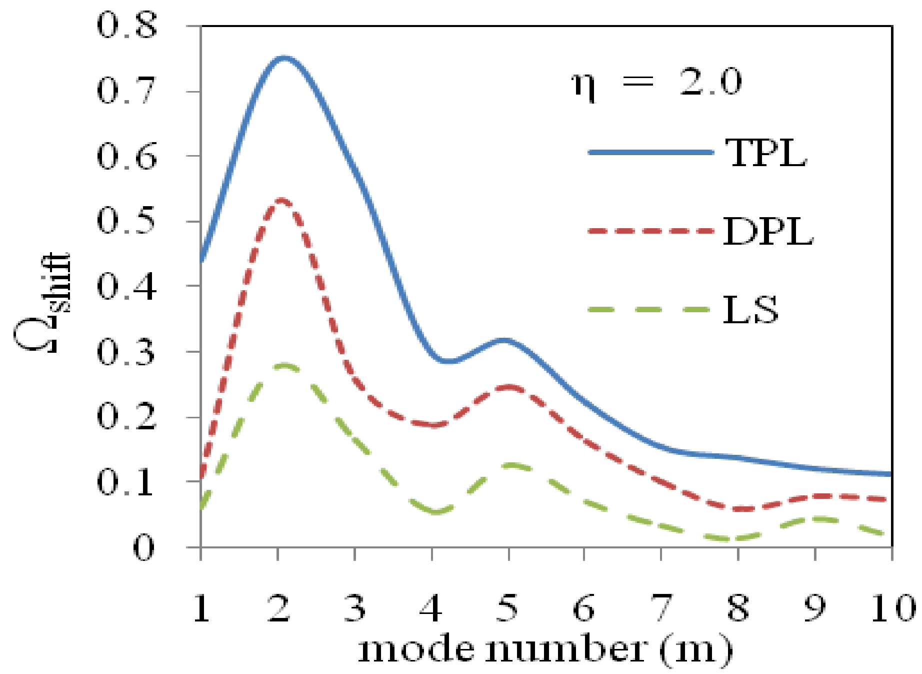

Figure 4.5(b): Frequency shift (Ω_{Shift}) against mode number (m) for TPL, DPL and LS models at $\eta = 2.0$ in nonlocal thermoelastic hollow cylinder with voids without magnetic field.

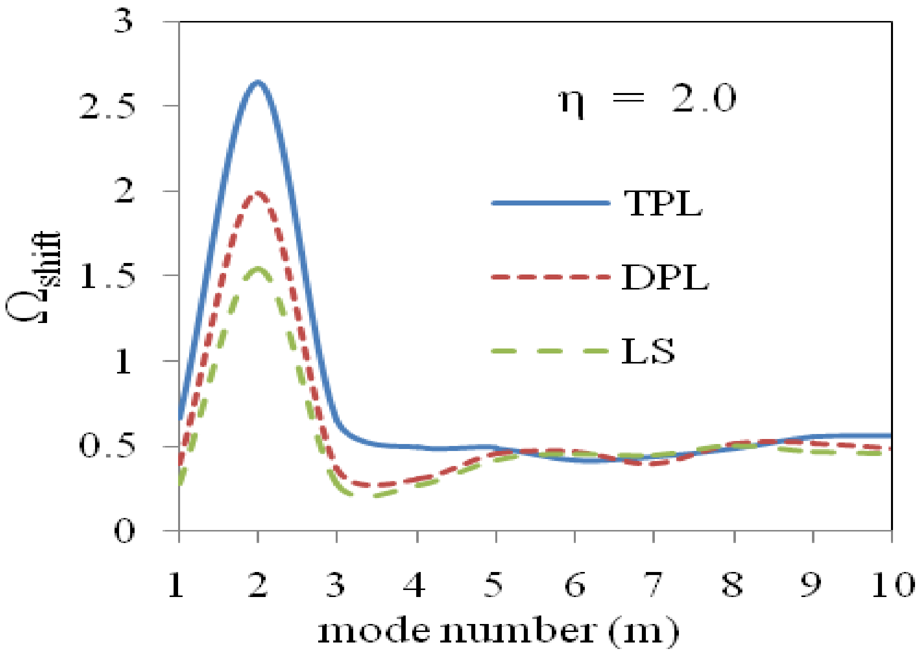

Figure 4.6(a): Frequency shift (Ω_{Shift}) against mode number (m) for TPL, DPL and LS models at $\eta = 2.0$ in local thermoelastic hollow cylinder with voids with magnetic field.

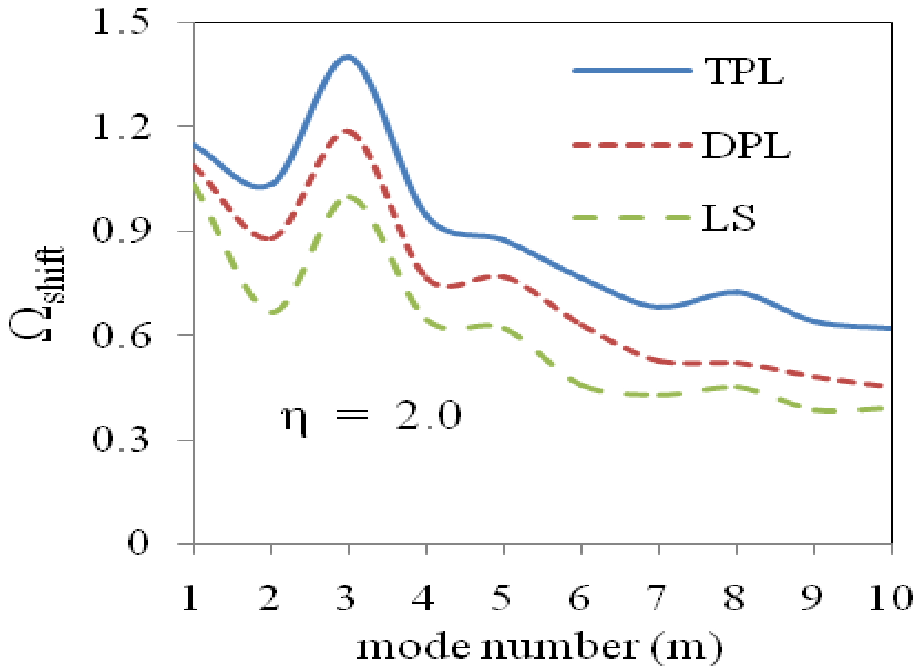

Figure 4.6(b): Frequency shift (Ω_{Shift}) against mode number (m) for TPL, DPL and LS models at $\eta = 2.0$ in local thermoelastic hollow cylinder with voids without magnetic field.

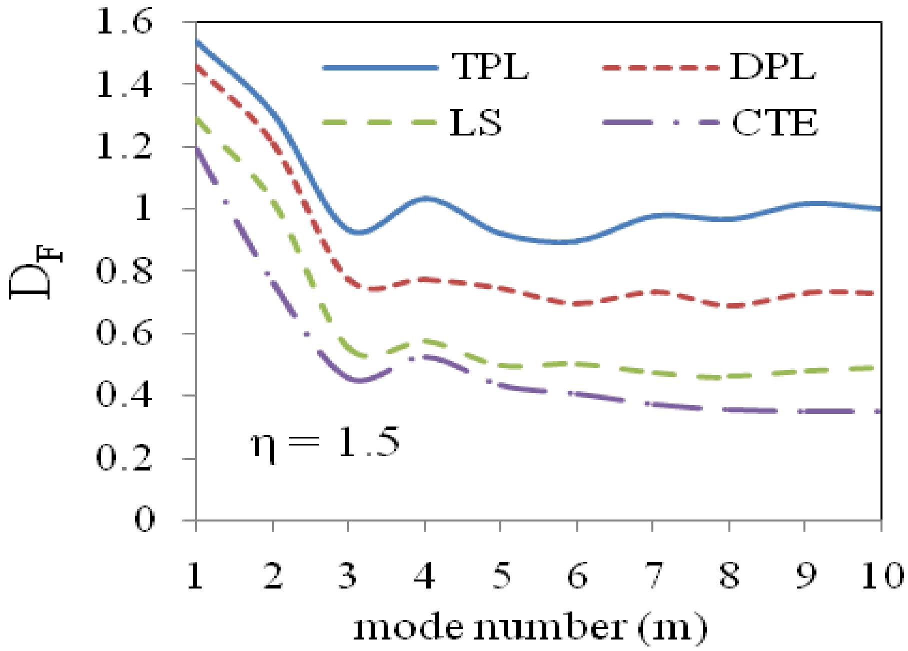

Figure 4.7(a): Thermoelastic damping (D_F) against mode number (m) for TPL, DPL, LS and CTE models at $\eta = 1.5$ in nonlocal thermo-elastic hollow cylinder with voids with magnetic field.

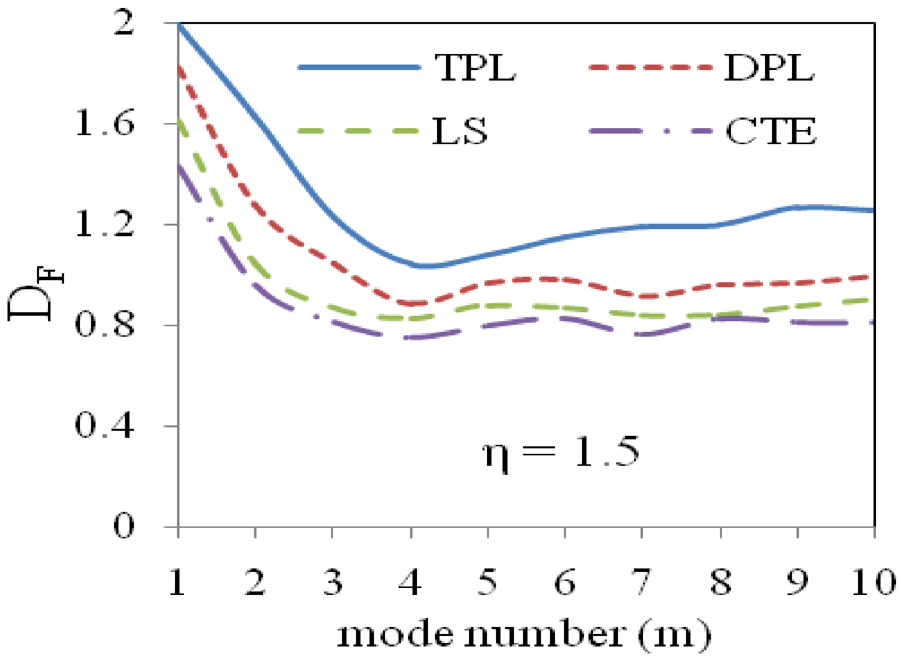

Figure 4.7(b): Thermoelastic damping (D_F) against mode number (m) for TPL, DPL, LS and CTE models at $\eta = 1.5$ in nonlocal thermo-elastic hollow cylinder with voids without magnetic field.

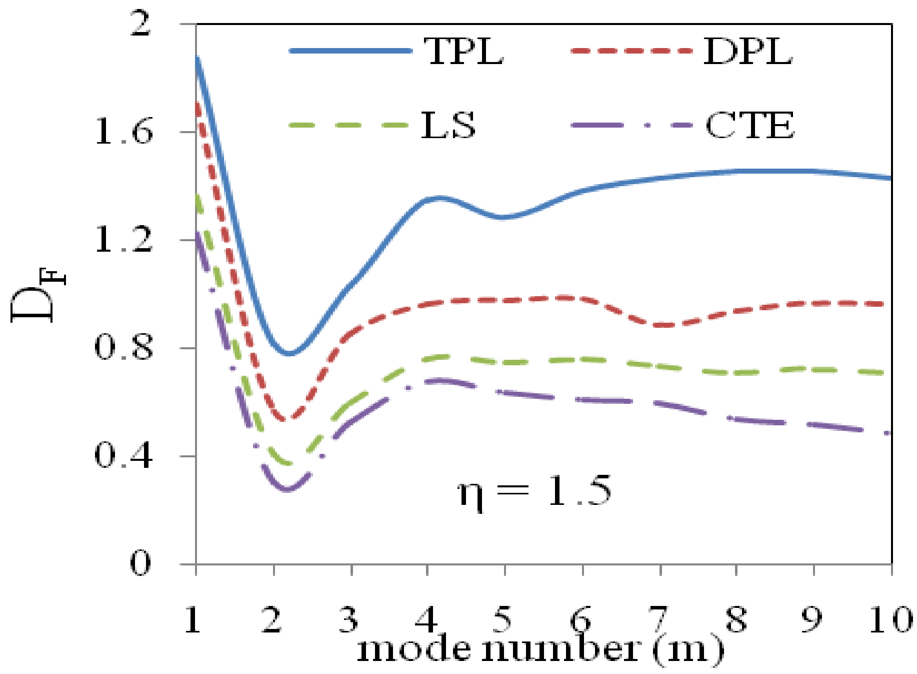

Figure 4.8(a): Thermoelastic damping (D_F) against mode number (m) for TPL, DPL, LS and CTE models at $\eta = 1.5$ in local thermo-elastic hollow cylinder with voids with magnetic field.

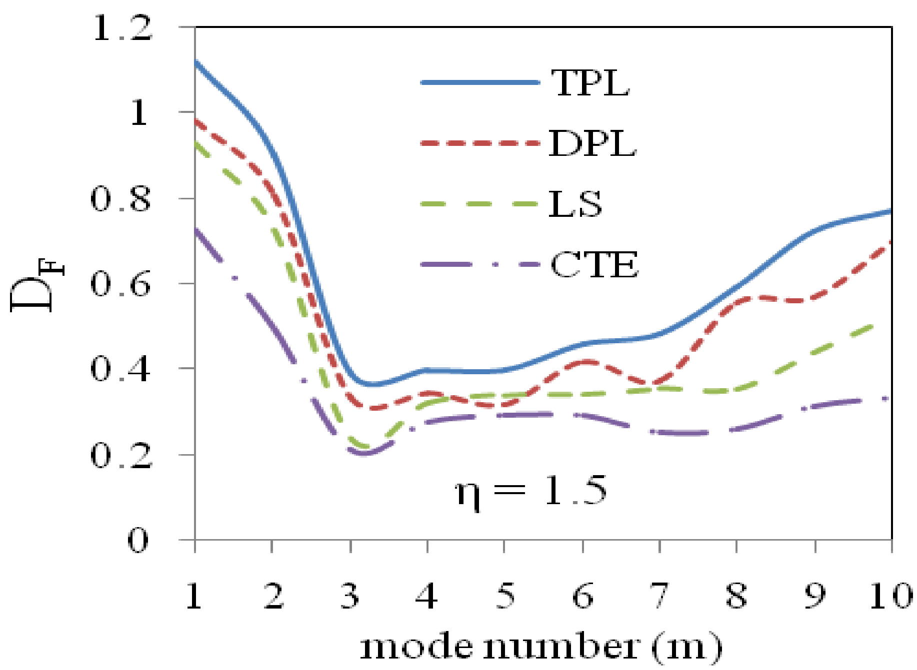

Figure 4.8(b): Thermoelastic damping (D_F) against mode number (m) for TPL, DPL, LS and CTE models at $\eta = 1.5$ in local thermo-elastic hollow cylinder with voids without magnetic field.

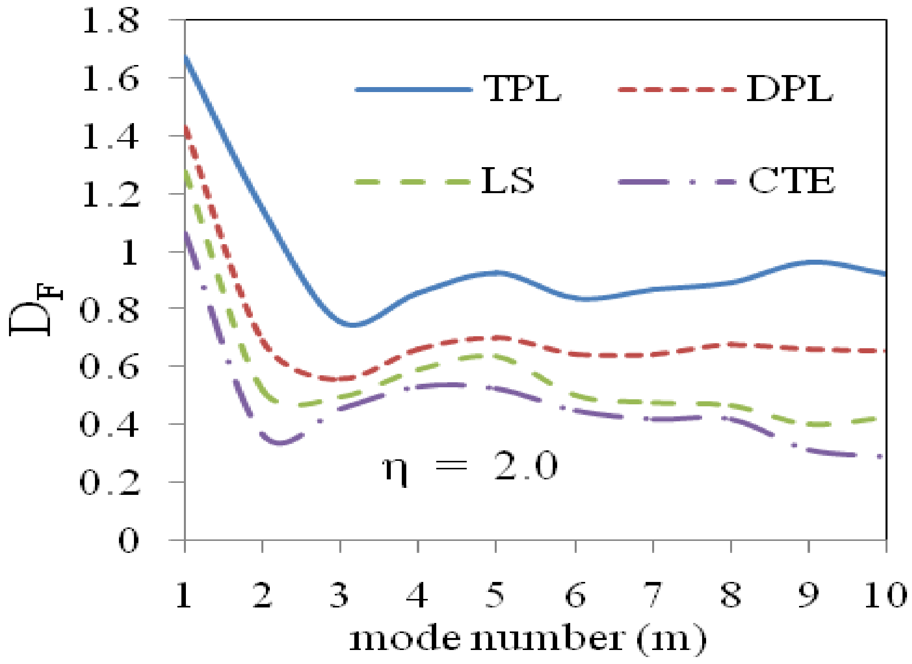

Figure 4.9(a): Thermoelastic damping (D_F) against mode number (m) for TPL, DPL, LS and CTE models at $\eta = 2.0$ in nonlocal elastic hollow cylinder with voids with magnetic field.

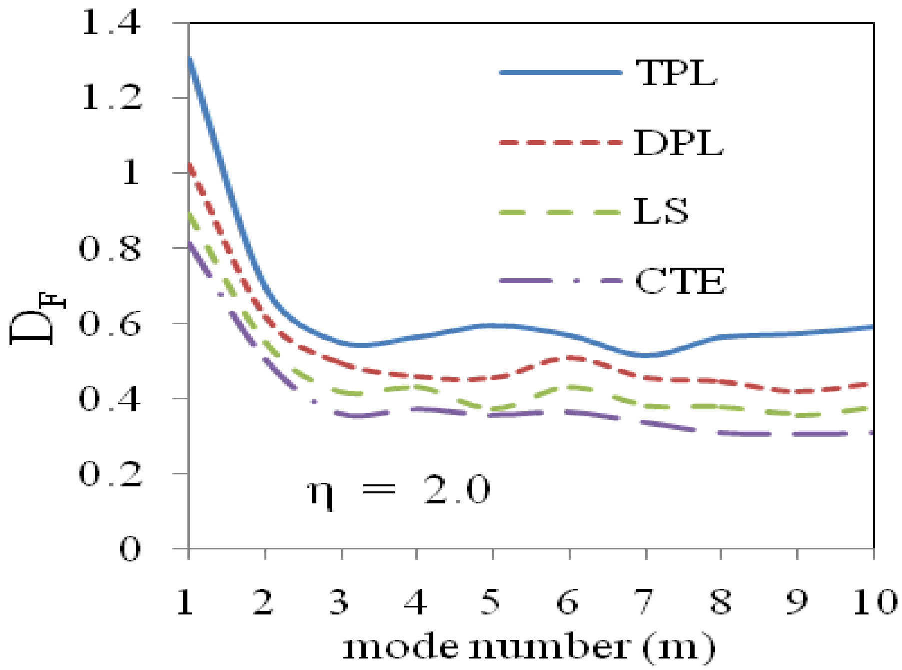

Figure 4.9(b): Thermoelastic damping (D_F) against mode number (m) for TPL, DPL, LS and CTE models at $\eta = 2.0$ in nonlocal elastic hollow cylinder with voids without magnetic field.

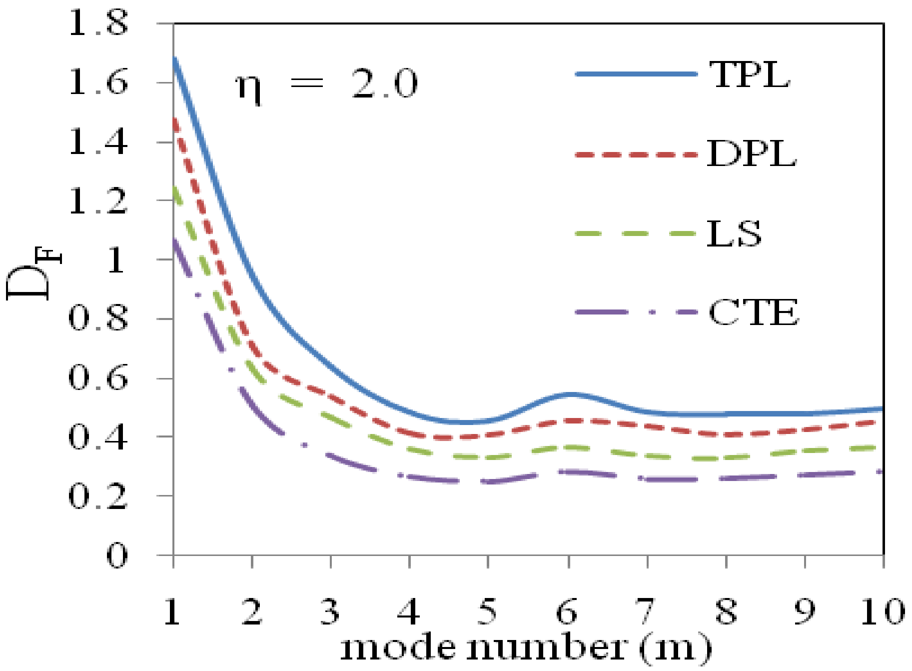

Figure 4.10(a): Thermoelastic damping (D_F) against mode number (m) for TPL, DPL, LS and CTE models at $\eta = 2.0$ in local thermo-elastic hollow cylinder with voids with magnetic field.

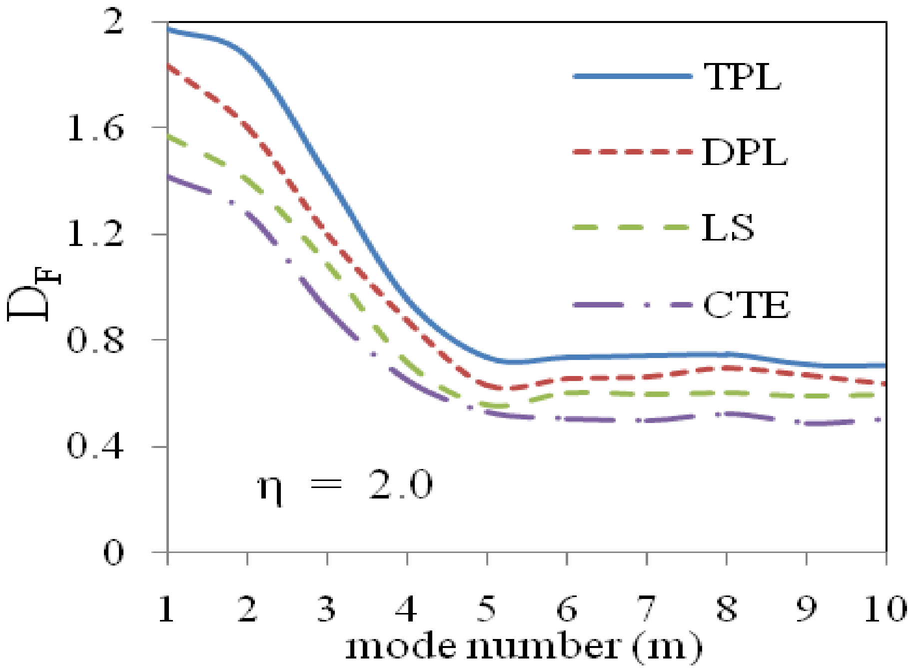

Figure 4.10(b): Thermoelastic damping (D_F) against mode number (m) for TPL, DPL, LS and CTE models at $\eta = 2.0$ in local thermo-elastic hollow cylinder with voids without magnetic field.

The frequency shift (Ω_{shift}) and the thermo-elastic damping related to inverse quality factor (Q^{-1}) for transversely isotropic electro-magneto generalized thermoelastic hollow cylinder have been calculated by Moosapour et al. (2014) as :

$$\Omega_{shift} = \left| \frac{\Omega_R^{\Upsilon^*} - \Omega_R^{CTE}}{\Omega_R^{CTE}} \right| , \quad Q^{-1} = 2\left| \frac{\Omega_I}{\Omega_R} \right|$$

, Here CTE stands for coupled thermoelasticity and Υ^* denotes for LS, DPL, TPL models of generalized thermoelasticity. Here, in the figures thermoelastic damping has been denoted as $Q^{-1} = D_F$. Fig. 4.3 and Fig. 4.4 have been represented for frequency shift (Ω_{shift}) against mode number (m) for different models of generalized thermoelasticity i.e. TPL, DPL and LS at $\eta = 1.5$ for nonlocal/local elastic cylinders with voids in presence/absence of magnetic field. It is observed from Figs. 4.3(a–b) (nonlocal case with/without magnetic field) that initially the variation of frequency shift vibrations is lower, the peak values have been noticed at $m = 2.0$, and keep on decreasing linearly with increasing value of mode number. This has been noticed from Fig. 4.4(a) (local with magnetic field) that the frequency shift vibrations are lower initially, accomplish maximum amplitude at $2.0 \le m \le 4.0$ and with increasing values of m, the behavior of vibrations goes on decreasing and become linear after $m = 7.0$. Fig. 4.4(b) (local without magnetic field) shows that initially vibrations have lower behavior, accomplish maximum amplitude at $m = 2.0$, then decreases to attain small peaks at $m = 4.0$ and go on decreasing to become linear at $m = 6.0$.

The frequency shift is represented in Fig. 4.5 and Fig. 4.6 for TPL, DPL and LS models of generalized thermoelasticity at $\eta = 2.0$ for nonlocal/local elastic voids hollow cylinder with/without magnetic field. It has been observed from Figs. 4.5(a–b) that initially the frequency shift vibrations are low, after attaining its maximum amplitude at $m = 2.0$, it decreases slightly at $m = 4.0$ and keep on decreasing linearly with increasing mode number. It is revealed from Fig. 4.6(a) that the behavior of frequency shift vibrations is low initially, attain its peak value at $m = 2.0$, decreases up to $m = 3.0$ and become linear with an increase in value of m. Fig. 4.6(b) tells that initially the frequency shift vibrations are meager, attains its maximum amplitude between $2.2 \le m \le 4.3$, and keep on decreasing with increase in mode number. This is to be noticed that the variation of vibrations are larger in TPL case than DPL and LS cases.

The thermoelastic damping (D_F) against mode number (m) have been drawn in Figs. 4.7 and 4.8 for the generalized thermoelastic models, i.e. TPL, DPL, LS and CTE at $\eta = 1.5$ for nonlocal/local elastic cylinder with voids in presence/absence of magnetic field. This is noticed from Figs 4.7(a–b) (nonlocal case) that initially the thermoelastic damping vibrations are larger, go on decreasing up to $m = 3.0$ and from left to right, the variation of vibrations becomes linear. It has been revealed form Fig. 4.8(a) (local case with magnetic field) depict that initially the thermoelastic damping vibrations are larger, achieve its minimum amplitude between $2.0 \le m \le 3.0$, increases up to $m = 4.0$ and with increasing mode number values, the vibrations become linear. Fig. 4.8(b) (local case without magnetic field) tells that initially the vibrations are larger, decreases up to $m = 3.0$, and with increasing values of mode number, the vibrations keep on increasing linearly.

The thermoelastic damping (D_F) versus mode number (m) has been represented in Figs. 4.9 and 4.10 for TPL, DPL, LS and CTE models of thermoelasticity at $\eta = 2.0$ for nonlocal/local elastic hollow cylinders with voids in presence/absence of magnetic field. It is concluded from Figs. 4.9(a–b) (nonlocal case) that initially the variation of thermoelastic damping vibrations is larger, decreases up to $m = 3.0$ and with increasing values of mode number the vibrations become linear. It has been noticed from Fig. 4.10(a) (local case) that initially the thermoelastic damping vibrations are larger, decreases up to $m = 4.5$, and with increasing values of m, the vibrations become linear. This is observed from all the figures that the vibrations are larger in case of TPL model in comparison with DPL, LS and CTE models of thermoelasticity. Also due to the effect of magnetic field the behavior of vibrations is noted to be larger without magnetic field in contrast to with magnetic field. It is observed that thermoelastic damping vibrations noted to be decreasing between $m = 3.0$ to $m = 5.0$ and then become linear**.**

4.7 Conclusions

Vibration analysis of electro-magneto transversely isotropic generalized nonlocal thermoelastic hollow cylinder with voids material has been presented in the reference of TPL model**.** The outer and inner surfaces of hollow cylinder have been assumed stress free and thermally insulated/isothermal**.** From the discussion of analytical and numerical results, following conclusions have been observed:

1. It is clearly indicated from the effect of magnetic field that the variations are larger in absence of magnetic field in contrast to the presence of magnetic field.
2. The effect of TPL model of magneto thermoelastic hollow cylinder is presented numerically for field functions i.e. thermoelastic damping and frequency shift in presence/absence of magnetic field. All the figures depict that the variation of vibrations has larger behavior in the TPL model of generalized thermoelasticity in contrast to DPL. LS and CTE cases because of effect of phase-lags of relaxation time parameters.
3. It is observed from the analysis of graphs that the natural frequencies clearly indicate that as mode number increases, the vibrations go on increasing. This has been noticed that after attaining maximum and minimum amplitudes of variations, the behavior of thermoelastic damping becomes linear because of the coupling between elastic, voids equilibrated volume fraction and thermal fields.
4. The free vibration functions i.e. thermoelastic damping and frequency shift are influenced by non-locality effect and represented for nonlocal and local cases with/without magnetic fields. From present work, researchers may receive the motivation to inspect the analysis of free vibrations of thermoelastic and magneto-thermoelastic materials with voids as novel applications in continuum mechanics such as material science, designing of new materials and useful in practical situations such as geomagnetic, optics, geophysics and acoustics, oil prospecting etc.
5. From literature study, it has been found that the TPL models provide better approach to allow voids and relaxation time parameters, which have many applications in the field of science, technology and engineering. This chapter gives useful applications in the area of seismology for mining and drilling in the earth's crust.